Soil N availability, rather than N deposition, controls indirect N_2O emissions

M.R. Redding [a, *], P.R. Shorten [b], R. Lewis [a], C. Pratt [a], C. Paungfoo-Lonhienne [c], J. Hill [a]

[a] Department of Agriculture and Fisheries, PO Box 102, Toowoomba, Queensland, Australia
[b] AgResearch Limited, Ruakura Research Centre, Private Bag 3123, Hamilton, New Zealand
[c] School of Agriculture and Food Sciences, The University of Queensland, St. Lucia, QLD, 4072, Australia

ARTICLE INFO

ABSTRACT

Ammonia volatilised and re-deposited to the landscape is an indirect N_2O emission source. This study established a relationship between N_2O emissions, low magnitude NH_4 deposition (0–30 kg N ha^{-1}), and soil moisture content in two soils using in-vessel incubations. Emissions from the clay soil peaked (< 0.002 g N [g soil]$^{-1}$ min^{-1}) from 85 to 93% WFPS (water filled pore space), increasing to a plateau as remaining mineral-N increased. Peak N_2O emissions for the sandy soil were much lower ($< 5 \times 10^{-5}$ µg N [g soil]$^{-1}$ min^{-1}) and occurred at about 60% WFPS, with an indistinct relationship with increasing resident mineral N due to the low rate of nitrification in that soil. Microbial community and respiration data indicated that the clay soil was dominated by denitrifiers and was more biologically active than the sandy soil. However, the clay soil also had substantial nitrifier communities even under peak emission conditions. A process-based mathematical denitrification model was well suited to the clay soil data where all mineral-N was assumed to be nitrified ($R^2 = 90\%$), providing a substrate for denitrification. This function was not well suited to the sandy soil where nitrification was much less complete. A prototype relationship representing mineral-N pool conversions (NO_3^- and NH_4^+) was proposed based on time, pool concentrations, moisture relationships, and soil rate constants (preliminary testing only). A threshold for mineral-N was observed: emission of N_2O did not occur from the clay soil for mineral-N <70 mg (kg of soil)$^{-1}$, suggesting that soil N availability controls indirect N_2O emissions. This laboratory process investigation challenges the IPCC approach which predicts indirect emissions from atmospheric N deposition alone.

1. Introduction

Ammonia-N is volatilised from a wide range of human production systems and activities including animal production (intensive and extensive), sewage treatment, and manure or inorganic fertiliser application to land. Ammonia, although not itself a greenhouse gas (GHG), has the potential to form nitrous oxide (N_2O). Ammonia volatilisation sources are therefore recognised in GHG inventory calculation protocols (IPCC, 2006). Ultimately, much of the volatilised ammonia is assumed to be deposited from the atmosphere onto land and ocean surfaces. Data suggests that some of this deposition can be relatively close to the source. For example, ammonia volatilisation from cattle feed yards results in adjacent nitrogen deposition, sometimes peaking within 75 m of the source (Todd et al., 2008). However, it appears that most of the volatilised ammonia (90%) is advected away from the source. In one study only 10% was deposited (dry deposition) within 4 km of the source (Staebler et al., 2009). This estimate was similar to those of a previous study, where 3–10% of volatilised ammonia from a poultry shed was observed to be deposited within 300 m of the source (Fowler et al., 1998).

The factor for secondary N_2O emissions from deposited ammonia employed by the IPCC, 0.01 (kg N_2O − N)(kg NH_3^+ − N volatilized)$^{-1}$ (IPCC, 2006), was based on a limited range of northern hemisphere studies. Two key studies involved the measurement of N_2O emission from forest soils in Germany (Butterbach-Bahl et al., 1997; Brumme et al., 1999), another included a literature review and calculations based on Netherlands-specific scenarios (Denier and Bleeker, 2005). Within the inventory guidelines (IPCC, 2006) there is recognition that low

* Corresponding author.
E-mail address: matthew.redding@daff.qld.gov.au (M.R. Redding).

deposition rates lead to low indirect emissions rates (based on measurements from low ammonia depositions in Canada; Corre et al., 1999), and a lower emission factor may be appropriate (page 11.24, IPCC, 2006). The accuracy of this approach for varied agricultural systems in other locations is unknown, and all of the cited studies assumed ammonia deposition rates based on literature values (Pratt et al., 2015). However, actual measurement of ammonia deposition rates suggests that these rates exhibit large spatial variability. This variability may be dependent on the proximity to land uses that are strong volatilisation sources e.g. industrial processes, intensive livestock production, and sewage treatment (IPCC, 2006).

However, deposition rate is unlikely to be the only controlling influence on these indirect N_2O emissions. A wide range of geochemical factors are known to influence the microbial communities ultimately responsible for N_2O emission from soils. These include soil moisture (Firestone et al., 1989; Davidson et al., 1991, 2000), temperature (Dobbie and Smith, 2001), oxygen supply, decomposable organic matter content, pH, and salinity (as reviewed by Dalal et al., 2003).

There is an unfilled niche for a systematic investigation of the influence of low magnitude ammonia deposition (rates that reflect common ammonia deposition of volatilised NH_4^+ in agricultural landscapes) and soil moisture conditions on N_2O emission intensity. This investigation seeks to fill this niche, collecting a high resolution laboratory data set of the interrelationship between moisture content, ammonia deposition, and their combined effect on N_2O emission for two soils. Our hypothesis is that the described influence of ammonia deposition rate (IPCC, 2006), and moisture content (Linn and Doran, 1984; Bouwman, 1998; Firestone et al., 1989; Davidson et al., 1991, 2000) on N_2O emission forms a continuous denitrification relationship that can be quantitatively characterised. As a tool to place the data in this context we use a modification of a previously published model (Xu et al., 1998) that relates N_2O emission to soil-resident mineral N (ammonia deposition plus pre-existing mineral-N) and moisture content (via a stress function, ranging from 0 to 1). Our studies also revealed several potential management approaches to decrease indirect N_2O emissions related to ammonia deposition or fertiliser use. It is intended that our research will help elucidate some of the key processes driving N cycling and GHG emissions relating to the connected concepts of soil, manure and fertiliser management. Indeed, as pointed out by Butterbach-Bahl et al. (2013), we still understand very little regarding these dynamics.

2. Materials and methods

2.1. Soil samples

Two soils representative of the surface 0.01 m of the profile were selected for the study and sampled with the permission of the private land owners. Both soils were from the Darling Downs of Queensland, but of very different character. The sandy soil was collected from the A horizon of a Natrustalf (Soil Survey Staff, 1998), classified as a Grey Sodosol soil in the Australian Soil Classification (Isbell, 2002). A self-mulching expanding clay soil, typical of the highly productive broad acre cropping areas of the Darling Downs was also collected. This soil was classified as a Vertisol (Soil Survey Staff, 1998) and a Black Vertosol using the Australian Soil Classification (Isbell, 2002).

Soil samples were sieved to pass a 2 mm mesh, representing the disruption associated with cultivation at the sites, and retained in the field moist condition. The following analytical techniques as set out in Rayment and Lyons (2010) were applied to the two soil samples collected: pH in 1:5 soil:water suspension (Method 4A1);

electrical conductivity (EC; Method 3A1); 2 M KCl extractable ammonium-N (NH_4^+-N) and nitrite + nitrate-N by steam distillation ($NO_3^- + NO_3^-$ N; Method 7A1); total N by Dumas high temperature oxidation (Method 7A5 and 6B2b); organic carbon (OC) content by the method attributed to Walkley and Black (1934); cation exchange capacity via alcoholic 1 M ammonium chloride (Method 15C1); particle size analysis of the soil samples was carried out using the hydrometer method described in Gee and Bauder (1986); moisture content was determined at 105 °C and reported on dry basis.

Surface soil (0.01 m) bulk density was estimated from repacked bulk density. Saturated water content was determined by slowly immersing a 500 ml Buchner funnel filled with the soil in distilled water, until the water level was coincident with the surface of the soil. The soil remained immersed for 8 h before the moisture content was determined based on the final weight less dry weight of the soil and Buchner funnel. This method allowed the clay soil to expand in response to the presence of water, allowing an estimate of 100% water filled pore space (WFPS).

2.2. Gas sampling and analysis apparatus

Two analysers were employed to obtain gas concentration data. This included a prototype FTIR closed path analyser (subsequently commercialised as a Spectronus FTIR Analyser) and a Cavity Ring Down Spectrophotometer (Picarro model 2130) allowed on-line analysis for CO_2 and N_2O (one analysis minute-1) and NH_3 (30 s average values delivered every half second).

Sample gas was supplied to these analysers at a flow rate of 2.5 l min^{-1} (all flow rates and gas volumes standardised to 101.325 kPa and 25 °C), via an automated gas flow manifold and a vacuum pump (12 V KNF diaphragm vacuum pump; www.knf. com). This flow manifold (Fig. 1) was constructed to sequentially deliver gas samples from 32, 1 L, vessels by opening and closing inlet and outlet valves (a total of 64 SMC solenoid valves; www. smcusa.com). The 64 solenoid valves were controlled by a single board computer (Technologics Systems Embedded Arm TS4200-8160; www.embeddedarm.com) using four 8-relay boards (Technologics Systems TS-Relay8). Gas flow was controlled by mass flow controller (Alicat MC series 10 L capacity; www.alicat.com) with flow rate set by the single board computer via serial communications (RS232 interface).
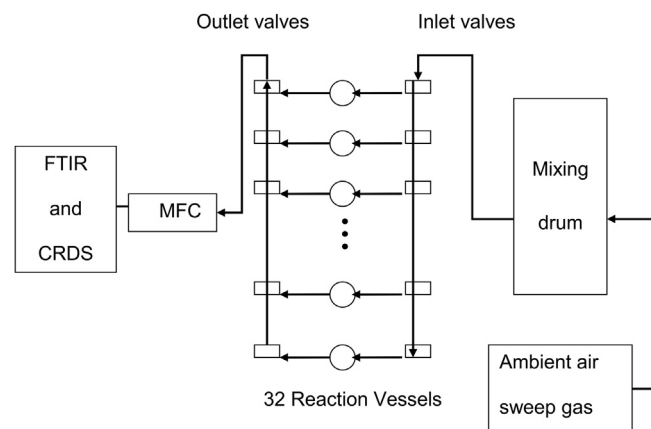

Fig. 1. Gas sampling and analysis layout. The system consists of a common sweep gas source (in this case ambient air), an array of inlet solenoid valves, reaction vessels, and outlet solenoid valves (32 of each), leading to a Fourier Transform Infrared Spectrophotometer (FTIR) and a Cavity Ring Down Spectrophotometer (CRDS). Flow rates (via mass flow controller; MFC) and switching are controlled by a single board computer.

The valve sequencing and MFC flow control were accomplished via python programming (Python Software Foundation, 2014), based on timing (correction via network time protocol) and serial communications from the Spectronus's valve control (RS485 protocol). A supply of sweep gas was connected in common to all 32 inlet valves (Fig. 1). For our experiments, ambient air was drawn through a 21 l mixing drum to the sweep gas inlet.

2.3. Experimental design

In summary, the treatment for each soil allowed N_2O emission measurement over a wide range of NH_4^+ deposition rates and moisture contents (air dry to 100% WFPS).

Treatments (from 0 to 30 kg of NH_4^+-N ha^{-1}) were selected to be representative of deposition over several months within a few hundred metres of a feedlot (Staebler et al., 2009) and assuming deposited N is retained in a soil depth of 0.01 m. Particular attention was directed at collecting high resolution data at lower application rates. In practice this involved applications of 0, and 0.000169–0.0202 g NH_4^+-N rising in a geometric series. These treatments were applied to 64 g of the clay soil and 84 g of the sandy soil (based on bulk density of the surface of the self-mulching vertosol of 0.95 kg l^{-1}; and 1.24 kg l^{-1} for the sandy sodosol soil) in 92 mm diameter cylindrical reaction vessels (2 L) in the form of ammonium chloride solution. Ammonium chloride is a common atmospheric ammonia aerosol (Pilinis and Seinfeld, 1987; Allen et al., 1989; Wexler and Seinfeld, 1990). Solution concentrations were formulated such that additions raised the WFPS of the soils to the targeted water contents (65 and 100% WFPS; 0 kg of NH_4^+-N ha^{-1} plus 14 deposition levels for 100% WFPS treatments, 0 kg of NH_4^+-N ha^{-1} plus 15 deposition levels for the 65% WFPS treatments). Each soil was examined in separate experiments, with one reaction vessel remaining empty to provide a blank (31 vessels with treated soil + blank). Additional treatments were subsequently completed for the clay soil, at two N deposition levels (0.0066 and 0.0132 g NH_4^+-N) and seven initial moisture contents between 64 and 96% WFPS.

Room temperature was controlled to 25 ± 2 °C, and bottle mass was monitored to assess the moisture content of each vessel every second day. Valve sequencing was set to allow sweep gas through each vessel for 10 min, followed immediately by 10 min of flow through the blank (640 min cycle), with flow set to 2.5 l min^{-1}.

Ammonia and N_2O concentrations in the sweep gas flow were continuously monitored (an NH_4^+-N measurement every three seconds and N_2O every minute). Remaining mineral-N in each vessel was estimated continuously from the initial soil mineral-N forms, the NH_4^+-N additions, and measured emissions of NH_3 and N_2O. This estimation approach for remaining mineral-N was assessed via mass balance for each vessel at the completion of the experiment (using Dumas N, mineral-N, and the collected emission data). This data combined with the detailed monitoring of vessel mass allowed emission behaviour to be established over a detailed mineral-N versus moisture content matrix. Importantly, this minimized sample disturbance during the experiment period.

The emission measurement cycle was commenced a day before treatments and soils were added to the vessels. Measurements continued for a sufficient period for drying processes to allow emission measurements to be collected from saturated to air-dry soil conditions (37 days for the clay soil, 25 days for the sandy soil).

2.4. DNA sequencing of peak emission samples

Eight additional reaction vessels were prepared for each soil, identically prepared as for the emission experiment. These treatments were supplied with water applications and N rates observed to maximise N_2O emission. Moisture contents were maintained at these levels daily. Half vessels received N treatments as NH_4Cl while the remainder received N as KNO_3. Gas emissions were monitored as described above, with the exception that a nitrogen sweep gas was used for the KNO_3 treatment (rather than ambient air) to ensure anaerobic conditions. Sampling was conducted 5 days after commencement, a point where previous experimentation suggested N_2O was strongly evident. Samples were immediately placed in a cool box during transport from the experimental laboratory to the genomic laboratory and stored at -20 °C for isolation of DNA.

Total dsDNA was extracted from selected soil samples (0.25 g) using Mo Bio Powerlyser™ PowerSoil™ DNA isolation kits following manufacturers instructions (Mo Bio Laboratories, Inc., Carlsbad, CA, USA). To characterise bacteria and archaea communities, the small-subunit (SSU) region of 16S ribosomal DNA (rDNA) gene from bulk DNA extracted from soil samples was amplified using primers broadly targeting bacteria and archaea: 341F (5'-CCTAYGGGRBGCASCAG-3') and 806R (5'-GGACTACNNGGGTATC-TAAT-3'). To profile fungal communities, the fungal internal transcribed spacer (ITS) region was PCR-amplified using ITS1F (5'-CTTGGTCATTTAGAGGTAA-3') and ITS2R (5'-GCTGCGTTCTTCATC-GATGC-3') primers. Both 16S rDNA and ITS primers were modified on the 5'end to contain the Illumina Nextera Adaptor i5 & i7 Sequences. PCR was performed using AmpliTaq Gold 360 master mix (Applied Biosystems). Thermocycling conditions were as follows: 95 °C for 5 min; 29 cycles of 94 °C for 30 s, 50 °C for 60 s, 72 °C for 60 s; 72 °C for 7 min. Amplicons were purified using Ampure magnetic beads (Beckman Coulter). A secondary PCR with Illumina Nextera XT v2 indices and Hi-Fidelity Takara Taq was performed to index each amplicon. A unique index was used for each sample to identify sequencing reads to sample. Amplicons were purified again using Ampure magnetic beads. Purified amplicons were quantified using Picogreen (Invitrogen) fluorometry on the Quant Studio (Life Technologies). Samples were normalised by pooling variable volumes of each amplicon in to a final pool. Normalized samples were set up for qPCR (KAPA Biosystems kit) on the Quant Studio and then standardised to 4 nM prior to sequencing on the Illumina MiSeq with 2 × 300 bp PE V3 chemistry. Sequencing was performed by the Australian Genome Research Facility Ltd.

2.4.1. Accession numbers

Nucleotide sequence accession numbers. 16S rRNA gene and ITS region amplicon sequencing data were deposited in GeneBank (SRR2104394 and SRR2104399, respectively).

2.5. Emission modelling

Nitrous oxide emission processes were investigated in soil via modification of an existing soil process-based model (Water and Nitrogen Management Model; WNMM) (Xu et al., 1998; Li et al., 2007), selecting suitable parameters to better represent the system. These parameters are directly measurable, or determined by characterizing the statistical distribution of emission variability. The total rate of N_2O emission (μg (g soil)$^{-1}$ min^{-1}) can be described by (similar to Xu et al., 1998, with the temperature term removed):

$$q_{N_2O} = K_D f_w(W), \tag{1}$$

where K_D is the first-order emission coefficient (defined by the measured maximal emission for the system) and is determined by soil organic matter content, soil drainage, tillage applied, presence of manure, climate, the occurrence of pans and $f_w(W)$ is a water stress function (ranging from 0 to 1) representing the effects of

water stress via a relationship with the fraction of water filled pore space (W). Our function is:

$$f_w(W; \mu_w, \alpha, \beta) = N(W; \mu_w, \alpha, \beta)/N(0; 0, \alpha, \beta),$$

$$N(W; \mu_w, \alpha, \beta) = \frac{\beta}{2\alpha\Gamma(1/\beta)} \exp\left(-\left(\frac{|W - \mu_w|}{\alpha}\right)\right) \quad (2)$$

where W is the measured WFPS (as a fraction) and $N(W; \mu_w, \alpha, \beta)$ is the generalised normal distribution with mean μ_w (the measured WFPS representing peak emission) and measured variance of the emission peak $\sigma^2 = \alpha^2 \Gamma(3/\beta)/\Gamma(1/\beta)$, where Γ is the gamma function (α, β are the scale/shape parameters respectively). This equation also ensures that $f_w(W; \mu_w, \alpha, \beta) = 1$ when $W = \mu_w$. Note that when $\beta = 2$, equation (2) reduces to the normal distribution.

The effect of soil nitrate on the total rate of N_2O emission ($\mu g \ (g \ soil)^{-1} \ min^{-1}$) via denitrification can be described by

$$q_{N_2O} = K_D f_w(W)\left[NO_3^-\right], \quad (3)$$

where $[NO_3^-]$ is the measured nitrate content of the surface soil ($\mu g \ (g \ soil)^{-1}$). An incremental development of this model (equation (3)) allows a nitrate-dependent effect on the fraction of water filled pore space for peak emission (μ_w), α, β and the threshold effect of $[NO_3^-]$ on the N_2O emission rate to be described:

$$q_{N_2O} = K_D f_w(W; \mu_w - c_1 E, \alpha + c_2, \beta + c_3) \frac{\left[NO_3^-\right]^M}{\left[NO_3^-\right]^M + K^M},$$

$$E = \frac{K_D\left[NO_3^-\right]^M}{\left[NO_3^-\right]^M + K^M}, \quad (4)$$

where K_D is determined by the maximal N_2O emission rate (as an estimate of denitrification, subject to experimental validation), μ_w is the fraction of water filled pore space for peak emission at low $[NO_3^-]$, α is the scale parameter for low $[NO_3^-]$, β is the shape parameter for low $[NO_3^-]$, c_1, c_2, c_3 describe the effect of $[NO_3^-]$ on the fraction of water filled pore space for peak emission, the scale parameter and the shape parameter respectively, K is the $[NO_3^-]$ for half-maximal N_2O emission, and M determines the threshold effect of $[NO_3^-]$ on N_2O emission.

A model incorporating both nitrification and N_2O emission, with some similarities to that of Mary et al. (1998), was also developed to investigate the role of nitrification on emission and to characterise soils based on their emission potential. Mineral N was partitioned into pools of ammonium ($[NH_4^+]$) and nitrate ($[NO_3^-]$). Mineralisation of organic-N to mineral-N was assumed to be small relative to the mineral-N pool within the time-span of the experiment. The two pool model is described by the coupled ordinary differential equations:

$$\frac{dA}{dt} = \beta\delta(t - t_0) - K_N\left[NH_4^+\right] - g(t), \quad A(t = 0) = A_0$$

$$\frac{dN}{dt} = K_N A - K_D f_w(W)\left[NO_3^-\right], \quad N(t = 0) = N_0 \quad (5)$$

where K_N is the rate of nitrification (day^{-1}), β is the concentration ($\mu g \ (g \ soil)^{-1}$) of added mineral N at time t_0 (day), $\delta(t)$ is the Dirac delta function, W is the fraction of water filled pore space, K_D is the first-order emission rate coefficient (day^{-1}), f_w is a water stress function (equation (2)), $g(t)$ is the measured rate of ammonia volatilization, A_0 is the initial soil ammonium concentration

($\mu g \ (g \ soil)^{-1}$) and N_0 is the initial soil nitrate concentration ($\mu g \ (g \ soil)^{-1}$).

2.6. Bioinformatics

Paired-ends reads were assembled by aligning the forward and reverse reads using PEAR (Zhang et al., 2014) (version 0.9.5). Primers were trimmed using Seqtk (version 1.0). Trimmed sequences were processed using Quantitative Insights into Microbial Ecology (QIIME 1.8) (Caporaso et al., 2010) USEARCH (Edgar, 2010; Edgar et al., 2011) (version 7.1.1090) and UPARSE software. Using usearch tools sequences were quality filtered, full length duplicate sequences were removed and sorted by abundance. Singletons or unique reads in the data set were discarded. Sequences were clustered followed by chimera filtered using "rdp_gold" database as reference. To obtain number of reads in each operational taxonomic unit (OTU), reads were mapped back to OTUs with a minimum identity of 97%. Using Qiime taxonomy was assigned using Greengenes database for 16S rDNA reads (DeSantis et al., 2006) or Unite database (Unite Version 6 dated: 2 March 2015) for ITS reads (Koljalg et al., 2005) providing genus-level resolution of communities.

2.7. Statistics

Cumulate emission curves and parameter relationships for the collected data were fitted by non-linear regression (nls procedure in R; R Core Team, 2012). Surface splines and spline curves were fitted via loess techniques, each using R (Loess procedure in R; R Core Team, 2012). Models (equations (2)–(5)) were fitted to the nitrous oxide emission data using linear and nonlinear regression (Bates and Watts, 2007). Model residuals were analysed for homoscedasticity and normality. We assumed that the variances of the deviations in measurements within response variables were constant. Markov Chain Monte Carlo was used to determine the standard errors in the model parameters (Gilks et al., 1996). Model fit was assessed using the correlation, slope and intercept between the predicted and observed emission rate (Pieiro et al., 2008). Pearson product moment correlation coefficient and Kendall's tau were used to describe the correlation between predicted and observed emission. Calculations were performed in R and MATLAB (R Core Team, 2012; The Mathworks Inc., 2012).

3. Results

3.1. Nitrogen recovery

The losses of NH_3 from the treated samples ranged from a small to substantial proportion of the treatment additions (0.4–15% for the high clay vertosol; 0.2–20% for the sandy textured sodosol soil; refer to contrasting characteristics of the two soils, Table 1).

Table 1
Soil characteristics (mean ± standard deviation).

Analysis	Units	Clay soil	Sandy soil
pH		7.9 ± 0	6 ± 0.1
EC	dSm^{-1}	0.21 ± 0	0.03 ± 0
$NH_4^+ - N$	$mg \ kg^{-1}$	2.33 ± 0.25	0.81 ± 0.08
$NO_3^- - N$	$mg \ kg^{-1}$	33.86 ± 0.47	2.43 ± 0.32
Dumas N	%	0.114 ± 0.008	0.03 ± 0
Organic C	%	1.29 ± 0.04	0.48 ± 0.05
Sand	%	47 ± 1	93.3 ± 0.6
Silt	%	14 ± 0	3 ± 0
Clay	%	38.7 ± 0.6	6 ± 0
CEC	$cmol \ kg^{-1}$	31.3 ± 0.6	1 ± 0

Recoveries of added N, based on final mineral-N (the sum of NH_4^+ and $NO_3^- + NO_2^-$) plus emitted N referenced to the nil addition treatment, were close to complete ($95\pm28\%$ for the clay soil and $99 \pm 17\%$ for the sandy soil; mean $\pm$ standard deviation; calculated for the 14 treatments of each soil where soil analysis mineral-N exceeded nil treatment mineral N remaining by a factor of two, in order to overcome detection limit issues).

In the clay soil, despite initial addition of N as NH_4^+, only $5.9 \pm 0.1\%$ of resident soil mineral N was in that form at the end of the experiment. Unlike the clay soil, simulated deposition of $NH_4^- - N$ resulted in little nitrification in the sandy sodosol soil. Between 40 and 100% of the resident mineral-N persisted in the NH_4^+ form, and there was a strong relationship between added $NH_4^+ - N$ and final $NH_4^+ - N$ ($R^2 = 0.96$).

3.2. Dependence on WFPS and mineral-N

The three dimensional graphs of N_2O emission versus soil moisture and resident mineral N illustrate the process relationships between emission and these control factors (Figs. 2 and 3). Emissions from the clay soil tended to peak from 85 to 93% WFPS, increasing as mineral-N increased. Emissions of N_2O from the sandy soil peaked at a lower WFPS (about 60%).

A curvilinear trend of increasing N_2O emission with resident mineral-N is evident for the clay soil (Fig. 2). In contrast, no such relationship was observed for the sandy soil (Fig. 3). Kendall's tau values for the relationship between N_2O emission and NO_3^- concentrations under peak emission conditions (WFPS 55–65%) for the sandy soil suggested that emissions were significantly related to the final NO_3^- concentrations ($\tau = 0.23$, $P < 0.001$).

3.3. Nitrifier and denitrifier communities

Examination of the relative abundance of identified OTU's capable of nitrification and denitrification led to several general observations (Table 2). Denitrifiers were highly enriched in the clay soil under the trial conditions where ammonium was added to the soil ($3.87\pm1.74\%$ bacterial denitrifiers; $0.36\pm0.11\%$ fungal denitrifiers). The soil also contained a substantial concentration of bacterial nitrifiers ($2.54\pm0.33\%$; added ammonium), which is supported by the observed complete nitrification of added ammonium. Bacterial nitrifiers even persisted in the soil where only nitrate was added ($2.42\pm0.46\%$).

For the sandy soil, which was found to be significantly less biologically active than the clay soil ($P < 0.001$, T test, based on soil respiration from the initially saturated treatments; clay soil $1,434\pm342$ mg of $CO_2 (g\ soil)^{-1}$, n = 16; sandy soil 853 ± 128 mg of $CO_2 (g\ soil)^{-1}$, n = 16), results indicated a low presence of bacterial nitrifiers when ammonium was added to the soil ($0.61 \pm 0.13\%$). Relative abundance of fungal denitrifiers was markedly small ($0.21\pm0.16\%$), though bacterial denitrifiers were noticeably abundant in relative terms ($16.92\pm3.58\%$).

3.4. Model fit

Equation (4) was applied to the clay soil emission data, assuming that soil mineral N was retained entirely as NO_3^- (Figs. 2 and 4). The relationship between measured and model predicted N_2O emission from the clay soil is strong (equation (4); $R^2 = 0.90$, $P < 0.001$; Figs. 4 and 5). In this case, the estimated model parameters are $K_D = 0.00154\pm0.00018$ µg $(g\ soil)^{-1}\ min^{-1}$, $\mu_w = 0.896\pm0.016$ g water g^{-1}, $\alpha = 0.0137\pm0.0062$, $\beta = 2.11\pm0.68$, $c_1 = 0.0313\pm0.0182$, $c_2 = 0.0434\pm0.0170$, $c_3 = 1.64\pm1.41$, $K_D = 1.11 \times 10^{-4}\pm0.14 \times 10^{-4}$ µg $(g\ soil)^{-1}$, and $M = 4.13\pm0.98$. Though equation (4) does not conform closely to

the observed $NO_3^- - N$ concentration threshold for N_2O emission (Fig. 5), the fit further confirms that this threshold is statistically significant (M is significantly greater than 1; $P < 0.01$).

The model incorporating nitrification (equation (5)) was fitted to the combined 31 treatments for each soil. The estimated model parameters are $K_N = 0.91\pm0.26$ day^{-1}, $K_D = 0.0084\pm0.0026$ day^{-1}, $\mu_W = 0.875\pm0.008$ (g water) g^{-1}, $\alpha = 0.054\pm0.012$, $\beta = 2.50\pm0.58$, $A_0 = 11.69\pm2.63$ µg $(g\ soil)^{-1}$, and $N_0 = 22.04\pm2.66$ µg $(g\ soil)^{-1}$ for the clay soil and $K_N = 0.00024\pm0.000048$ day^{-1}, $K_D = 0.00019\pm0.000087$ day^{-1}, $\mu_W = 0.63\pm0.02$ (g water) g^{-1}, $\alpha = 0.22\pm0.05$, $\beta = 0.49\pm0.17$, $A_0 = 7.33\pm0.43$ µg $(g\ soil)^{-1}$, and $N_0 = 22.97\pm0.2$ µg $(g\ soil)^{-1}$ for the sandy soil. The rate of nitrification (K_N) is significantly greater in the clay soil than the sandy soil ($P < 0.001$) and the maximal rate of N_2O emission (an estimate of maximal denitrification rate, K_D, given the near complete N recovery values) is 45 times greater in the clay soil than the sandy soil ($P < 0.01$). The moisture dependent emission parameters (μ_W, α, β) are also significantly different between the clay soil and the sandy soil ($P < 0.01$).

The relationships between predicted (equation (5)) and observed $NO_3^- - N$ concentrations at the end of the trial were strong for the clay soil ($R^2 = 87\%$, the clay soil) though less satisfactory for the sandy soil (fit not significant for the sandy soil, due to NO_3^--N concentration being relatively close to zero). Final NH_4^+ concentrations were well predicted for the sandy soil ($R^2 = 98\%$, the sandy soil; fit not significant for the clay soil, due to $NH_4^+ - N$ concentration being relatively close to zero).

4. Discussion

4.1. Nitrogen recovery

In our study, resident treatment-N was approximated by the difference of treatment-N less the emissions ($NH_3 - N$ plus N_2O-N). This calculated value was validated using N recovery data from sample analysis after completion of the experiment. During method development and the conduct of the experiment any disturbance of the soil, even bumping the vessel, could result in erratic emission behaviour. Accordingly, soil sampling during the measurement period was not conducive to effective data collection and a different calculation approach to residual mineral-N was adopted. Neither mono nitrogen oxide (NO_x) nor N_2 losses were measured during the trial. While it is likely that some emission of these species did occur (Dalal et al., 2003), in this case mass balance suggests that these were small.

The estimation approach is also supported by default inventory values that suggest volatilisation of $NH_3 - N + NO_x - N$ from synthetic fertiliser application ranges from 3 to 30% of the total N applied (IPCC, 2006). Other studies indicate that the magnitude of NO-N losses are of the same order of magnitude as $N_2O - N$ emissions (Sanz-Cobena et al., 2012; Abalos et al., 2013), and are likely small relative to losses observed due to ammonia volatilisation (Stehfest and Bouwman, 2006; Yang et al., 2010). Some literature suggests that N_2 emissions are likely comparable to N_2O-N emissions as moisture contents approach saturation (Dalal et al., 2003), however, at lower moisture contents N_2O-N emissions dominate. Our mass balance data suggests that losses of the unmonitored species are likely small relative to the up to 20% observed loss of added N as NH_3.

4.2. N_2O emission dependence on WFPS and mineral-N

Emission values contributed a detailed three dimensional landscape representing N_2O emission dependence on WFPS and
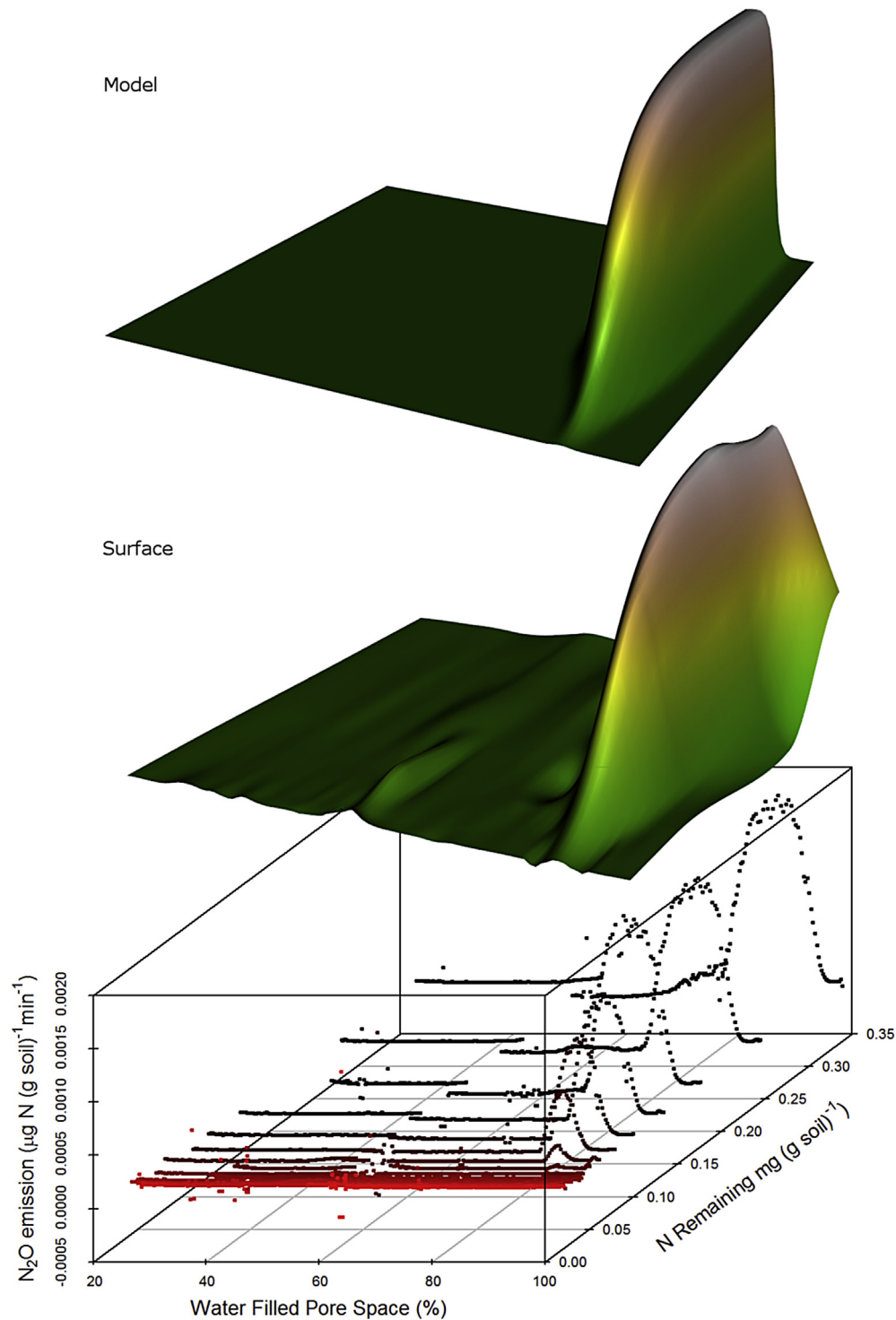
Fig. 2. Measured relationship between soil moisture (WFPS), mineral-N, and N₂O emission for the clay soil. A surface plot based on loess smoothing is superimposed to assist visualisation, in addition to the Equation (4) fit.

mineral-N (Figs. 2 and 3). Emissions from the clay soil tended to peak at higher moisture content than those from the sandy soil. The high moisture contents at peak emissions for the clay soil is consistent with the known effect of water filled pore space on oxygen supply limitation (Davidson et al., 1991; Dobbie and Smith, 2001; Dalal et al., 2003), a known driver of denitrification (Firestone et al., 1989; Khalil et al., 2004; Senbayram et al., 2009). For the clay soil, nitrification was almost complete at the end of the trial and N was dominantly in the form of NO_3^- (mean 95%, range 50—100%), providing the required substrate for denitrification. The relationship with mineral-N content for the clay soil (Fig. 2) is likewise consistent with the understanding that N₂O emission requires a source of mineral-N, and this emission becomes more prevalent compared to N₂ emission with a greater supply of NO_3^- (Swerts et al., 1996; Ball et al., 1997; Dalal et al., 2003).
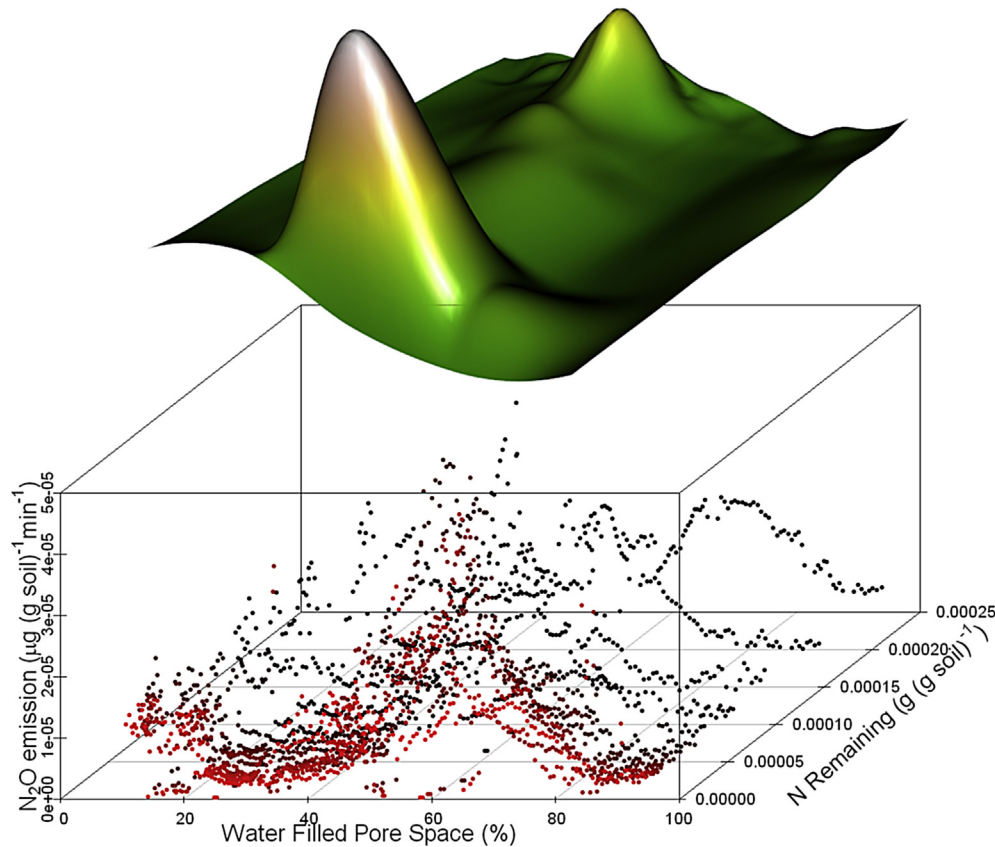
Fig. 3. Measured relationship between soil moisture (WFPS), mineral-N, and N$_2$O emission for the sandy soil. A surface plot based on loess smoothing is superimposed to assist visualisation.

Emission of N$_2$O also tended to increase as resident mineral-N increased in the clay soil, however, this was not the case for the sandy soil. Unlike the clay soil, simulated deposition of NH$_4^+$ − N resulted in little nitrification in the sandy sodosol soil. Suppression of nitrification has previously been partly attributed to high ammonia concentrations (Anthonisen et al., 1976), and this in turn may have contributed to the low N$_2$O emissions from this soil (compare emission scales, Figs. 3 and 4), though a more recent study questions this relationship (Hawkins et al., 2010). Moreover, soil factors such as organic C (Table 1), microbial diversity, and micronutrient status may also have caused different nitrification rates in the two soils. Emissions from the sandy sodosol soil (Fig. 3) are only a few percent of those from the clay soil, requiring analytical resolutions that were much closer to the limits of the FTIR instrument. It appeared that NH$_4^+$ added to the sandy soil was unrelated to the final NO$_3^-$ concentration (P ≈ 0.95; significance of correlation and Kendalls tau).

Emission conditions applied to the samples in the microbial community study corresponded to those that promoted maximal emission in the emission experiment (clay soil, 87% WFPS, 0.0202 g N sample^{-1}; sandy soil, 60% WFPS, 0.00505 g N sample^{-1}). In the clay soil under these conditions, where NH$_4^+$ − N was added to the soil, denitrifiers (dominated by non-fungal OTUs) were highly enriched. A substantial community of bacterial nitrifiers persisted whether NO$_3^-$ or NH$_4^+$ was added. However, the dominance of denitrifiers in the clay soil under both conditions, and the correspondence of near-saturation WFPS at peak emission suggests that denitrification dominates N$_2$O formation in this soil (Firestone et al., 1989; Khalil et al., 2004; Senbayram et al., 2009). Therefore the simultaneous and almost complete

nature of nitrification of added NH$_4^+$ − N in the emission trial may suggest on-going nitrification processes within aerobic soil microsites (Zanner and Bloom, 1995; Abbasi and Adams, 1998).

The sandy soil was significantly less biologically active and displayed a low presence of bacterial nitrifiers when ammonium was added to the soil, much of which remained as NH$_4^+$ − N at the completion of the experiment. The relative abundance of denitrifiers was markedly large in the sandy soil, being dominated by bacterial rather than fungal forms (Table 2). Nevertheless, the absolute populations of these organisms may be exaggerated by the relative abundances given the lower respiration of the sandy soil compared to the clay soil (sandy soil respiration about 60% of clay soil respiration). Taken together, the low respiration and the low nitrifier activity in sandy soil, producing little of the substrate for denitrification compared to clay soil, supports the low emissions of N$_2$O measured from the sandy soil compared to the clay soil. The relative abundance of denitrifiers in this soil, however indicates denitrification as the likely source of the small N$_2$O emission measured.

For both soils it is possible that nitrifiers contributed to emissions, despite the evidence for denitrification as the major source. Additionally, no data was collected as to the contribution of dissimilatory reduction of nitrate to ammonia, a fairly poorly quantified source of N$_2$O (as reviewed by Giles et al., 2012).

4.3. Modelling observed indirect N$_2$O emission processes

The denitrification model (equation (4)) conformed well to the clay soil emissions (Figs. 2 and 4), providing a quantitative relationship between WFPS, resident mineral-N, and N$_2$O emission. In

Table 2
The list of nitrifier and denitrifier relative abundance values in the vertisol and sodosol soils (absence indicated by "−"). All are the genus except for the class Thaumarchaeota (Brochier-Armanet et al., 2008) and the family Nitrospiraceae (Daims, 2014); Nitrospira and Nitrosovibri are well-known nitrifiers (Watson et al., 1989); Identification of denitrifiers is from Philippot et al. (2007) except for Trichosporon (Tsuruta et al., 1998).

Genus (%)	Clay soil		Sandy soil	
	NH$_4$	NO$_3$	NH$_4$	NO$_3$
Nitrifiers				
Thaumarchaeota	1.89 ± 0.22	1.89 ± 0.36	0.45 ± 0.07	0.48 ± 0.1
Nitrospiraceae1	0.06 ± 0.02	0.04 ± 0.01	0.03 ± 0.01	0.03 ± 0.02
Nitrospiraceae2	−	−	0 ± 0	0 ± 0
Nitrospira	0.56 ± 0.08	0.47 ± 0.08	0.13 ± 0.04	0.14 ± 0.03
Nitrosovibrio	0.03 ± 0.01	0.02 ± 0.01	0 ± 0	0 ± 0
Summary	2.54 ± 0.33	2.42 ± 0.46	0.61 ± 0.13	0.65 ± 0.16
Bacterial Denitrifiers				
Streptomyces	0.96 ± 0.3	0.89 ± 0.1	2.38 ± 0.27	3.2 ± 1.15
Alicyclobacillus	0.09 ± 0.05	0.1 ± 0.03	1.31 ± 0.09	2.07 ± 1.09
Bacillus	2.36 ± 1.25	3.27 ± 0.7	10.91 ± 2.53	13.86 ± 3.8
Paenibacillus	0.07 ± 0.03	0.09 ± 0.02	0.78 ± 0.23	0.84 ± 0.23
Hyphomicrobium	0.02 ± 0.01	0.02 ± 0.01	0.02 ± 0.02	0.02 ± 0.02
Mesorhizobium	0.15 ± 0.02	0.18 ± 0.01	0.27 ± 0.02	0.28 ± 0.05
Agrobacterium	0.06 ± 0.01	0.07 ± 0.02	0.03 ± 0.03	0.12 ± 0.19
Rhizobium	0.06 ± 0.02	0.07 ± 0.01	0.46 ± 0.27	0.38 ± 0.33
Azospirillum	0.06 ± 0.02	0.1 ± 0.02	0.02 ± 0	0.03 ± 0.02
Burkholderia	0.01 ± 0.01	0.01 ± 0.01	0.7 ± 0.1	0.88 ± 0.22
Acidovorax	0.01 ± 0.01	0.02 ± 0	0.01 ± 0	0 ± 0.01
Cupriavidus	0.01 ± 0	0.01 ± 0.01	0.03 ± 0.02	0.03 ± 0.02
Dechloromonas	−	0 ± 0	0.01 ± 0	0.01 ± 0
Pseudomonas	0.02 ± 0.01	0.01 ± 0.01	0 ± 0	0 ± 0
Summary	3.87 ± 1.74	4.85 ± 0.94	16.92 ± 3.58	21.71 ± 7.11
Fungal Denitrifiers				
Fusarium	0.36 ± 0.11	0.43 ± 0.16	0.21 ± 0.16	0.2 ± 0.13
Trichosporon	−	0 ± 0	−	−
Summary	0.36 ± 0.11	0.43 ± 0.16	0.21 ± 0.16	0.2 ± 0.13

isolation, the fit of the model to the observation is not strongly diagnostic that denitrification dominated N$_2$O emission processes rather than nitrification. However, the combined evidence of this model, the dominant population of denitrifiers, and the high
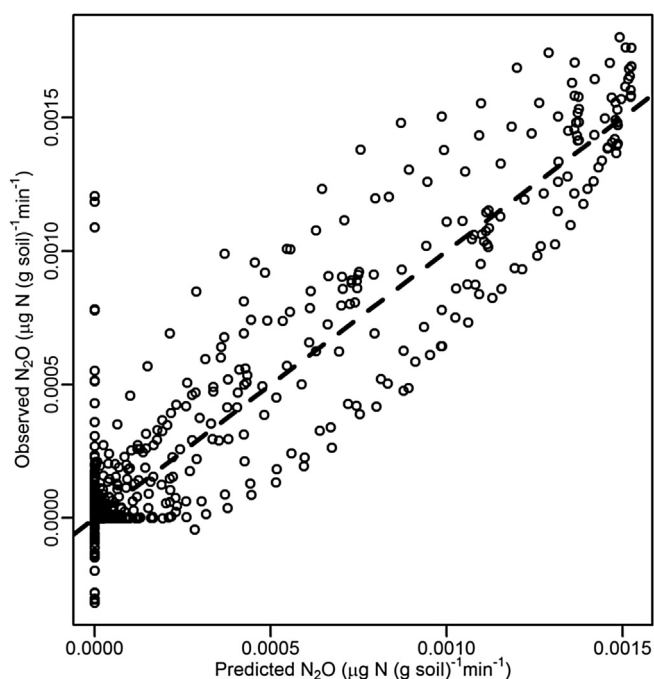

Fig. 4. Relationship between measured and model predicted N$_2$O emission (equation (4)) from the clay soil (R^2 = 0.90).
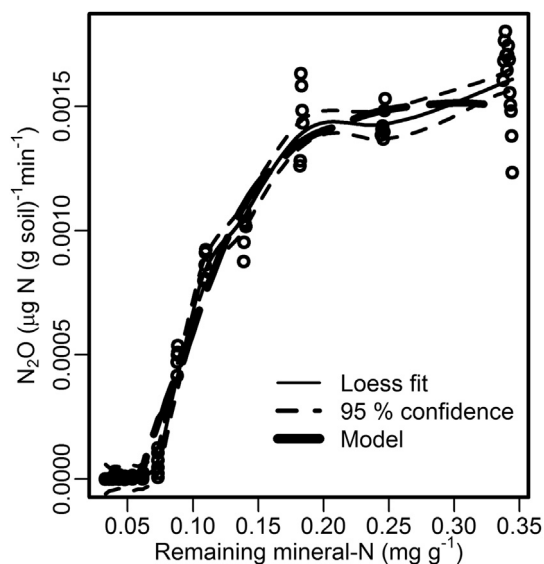

Fig. 5. A loess spline fitted to follow the peak values of the clay soil data (Fig. 2; peak WFPS ± 1%), illustrating that emissions do not significantly rise until >0.07 mg resident mineral-N g^{-1}. The spline (span 0.3) is bracketed by lines representing the upper and lower confidence interval of the mean (95%). The model (equation (4)) has also been plotted.

moisture content at peak emissions for this soil (Firestone et al., 1989; Khalil et al., 2004; Senbayram et al., 2009) all suggest that denitrification may be the major source of these emissions. It was evident during application of equations (1) and (2) that a good fit could only be achieved with this model by using a variable value of the emission coefficient (k_d, equation (1)), dependent on the moisture fraction for peak emission (μ_W), the scale parameter (α) and the shape parameter (β; linear relationships, P < 0.01). In particular, it was apparent (Fig. 2) that a model that quantified the relationships between peak emissions and WFPS, and the effect of nitrate concentration on the magnitude of peaks may better suit the data. Equation (4) has both of these characteristics, and conforms reasonably closely to the observed NO$_3^-$ − N concentration threshold for N$_2$O emission from the clay soil, where it is assumed that soil mineral N was retained entirely as NO$_3^-$ (Figs. 2, 4 and 5).

Nitrate-N concentrations in the clay soil were strongly dependent on the NH$_4^+$ − N treatment rate, and nitrification appeared almost complete. A WNMM-based model (Xu et al., 1998; Li et al., 2007) with the addition of a moisture dependent emission coefficient (k_d, equation (1)) was therefore a sound choice, and this was confirmed by the fit of equation (4) to the data.

Model fit to the sandy soil was less satisfactory, possibly because processes that emit N$_2$O were largely absent. Biological activity in the sandy soil was limited (respiration only 60% of that in the clay soil). Oxidation of NH$_4^+$ − N to NO$_3^-$ − N in the sandy soil is largely incomplete and microbial community data indicated the presence of a relatively small population of nitrifying organisms. These factors are reflected in the very low N$_2$O emission from this soil, though denitrifier community domination suggests that denitrification was the source of the small emission observed. Given this scenario, especially the limited transformation of NH$_4^+$ − N to the denitrification substrate NO$_3^-$ − N, it is unsurprising that equation (4) provided unsatisfactory fits: Equation (4) assumes added (and pre-existing) mineral-N is converted to NO$_3^-$.

Introducing a component to predict the degree of nitrification of mineral-N at a given point in time is perhaps the next step in producing a more generally applicable extension of equation (4). This approach was supported by correlation relationships between

N_2O emission and NO_3^- concentrations under peak emission conditions (WFPS 55–65%) for the sandy soil.

Though $NO_3^- - N$ concentrations were measured before treatment and at the completion of the experiment, progressive concentrations are not available. These initial and final data, however, provide an opportunity for a preliminary evaluation of the relationship proposed to predict $NO_3^- - N$ concentration (equation (5)). Importantly, the relationships between predicted (equation (5)) and observed $NO_3^- - N$ concentrations at the end of the trial were strong for the clay soil though less satisfactory for the sandy soil (though final NH_4^+ concentrations were well predicted for this soil). While these results are positive, further development of this model is required, preferably with incremental analysis of mineral-N species over time.

4.4. Implications

Nitrous oxide emission from soil proceeds only during the process of nitrate or nitrite formation (nitrification emission) or following nitrification processes (denitrification, assimilatory nitrate reduction, and abiotic nitrate/nitrite reduction) (Dalal et al., 2003). The ammonia deposition simulated in our study aligns well with these findings: a sandy soil with little nitrate formation resulted in little emission, while a strongly nitrifying clay soil displayed strong emissions and a clear relationship between nitrate concentration and emission. Validation of a nitrification relationship (e.g. equation (5)) would strengthen the ability of equation (4) to predict the lower emissions from poorly nitrifying soils. However, using ammonia deposition as a surrogate for final nitrified mineral-N in equation (4) is an effective representation of a worst-case scenario, in terms of emission losses.

Nitrous oxide emission from soil is also strongly related to soil moisture content. This is evident from published literature (Dobbie and Smith, 2001) and for both of the soils we studied.

Applying equation (4) to the soil moisture data collected from the clay soil (Redding et al., 2015; moistures measured for 12 months at a depth of 75 mm using an in-soil moisture probe), enables prediction of emission factors for a range of resident mineral-N scenarios, conservatively assuming that all mineral-N occurs as NO_3^- and a temperature of 25 °C (Fig. 6). The calculations for this figure hinge on the assumptions that deposited mineral-N and moisture are distributed homogeneously to a specific depth (Fig. 6, panel B). While we are constrained by these caveats of the data set, it nonetheless provides a valuable example of how this type of model can be applied. Note that the peak emissions of panel B (proportional emission versus resident mineral-N per area) are limited by the emission plateau of Fig. 2. Therefore proportional emissions in panel B tend to peak then decline.

This exercise highlights the critical importance of the mixing depth of nitrate in the soil where equation (4) is applied to calculate emissions from areas of land. While the distribution of mineral-N in soil profiles has been widely measured (e.g. Koehler et al., 2012), it is controlled by site specific factors: management, climate, and variation with time and in space. Given a 75 mm homogeneous mixing depth of deposited $NH_4^+ - N$, the range of mineral-N concentrations modelled (Fig. 6, panel B) corresponds to 0–249 kg resident mineral-N ha^{-1} (assuming soil upper cultivated layer bulk density is 950 kg N ha^{-1}), with emission maximising as a proportion of resident mineral-N at around 130 kg ha^{-1}. Resident mineral N of less than about 50 kg N ha^{-1} would result in no significant indirect N_2O emission (the threshold effect; 70 mg [kg of soil]$^{-1}$, Figs. 5 and 6). A different scenario, with a mixing depth of 10 mm would result in emission maximising at a resident mineral-N concentration of about 20 kg ha^{-1}.
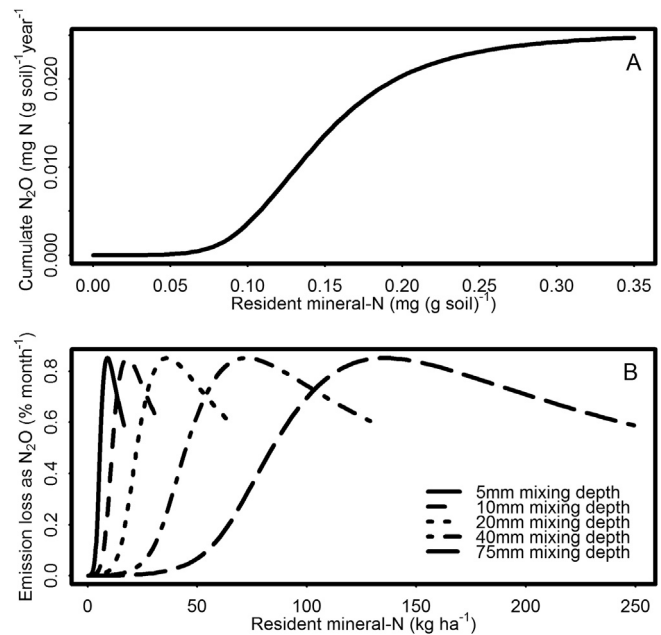

Fig. 6. Maintaining lower surplus mineral-N in the soil decreases N_2O emissions. Application of equation (4) to one year of clay soil moisture data collected from the field (Redding et al., 2015), for a range of resident mineral N values (panel A). This relationship is then applied to a range of hypothetical resident mineral-N scenarios and for different depths of homogeneous mixing (panel B).

Human influenced annual atmospheric N deposition values have been measured, finding that most of the NH_4^+ volatilised from these sources is likely to be advected away. In one study only 10% was deposited (dry deposition) within 4 km of the source (Staebler et al., 2009). A preceding study found that as little as 3–10% of volatilised NH_3 from a poultry shed was deposited within 300 m of the source (Fowler et al., 1998). In these scenarios, the advected plume of dispersing NH_4^+ may be re-deposited to the wider landscape, which will include a mosaic of less fertile areas and more intensively managed agricultural land. This diluted deposition would result in emissions that may be largely dependent on the soil initial $NO_3^- - N$ status rather than the deposition rate. Where deposition occurs to the clay soil resulting in resident mineral-N of less than 70 mg kg^{-1}, negligible N_2O emission will result (under the conditions investigated).

Close to the source, higher ammonia deposition rates are observed. Within 700 m of a poultry barn deposition of 42–68 kg N ha^{-1} $year^{-1}$ has been observed (Berendse et al., 1988). Based on deposition traps sited immediately downwind of four beef feedlots (7–14 day measurements), deposition of 29–172 kg N ha^{-1} $year^{-1}$ was observed (McGinn et al., 2003). Average deposition within 400 m of a feedlot, based on several aerial surveys, was estimated at equivalent to 254 kg N ha^{-1} $year^{-1}$ (Staebler et al., 2009). In another feedlot study, deposition was <49 kg N ha^{-1} $year^{-1}$ within 550 m of beef feedlot boundary, maximising at 75–106 m (Todd et al., 2008). Given that 90% of the volatilized NH_4^+ is advected away (and perhaps ultimately deposited over a much larger area), these values probably over-estimate the median deposition rates.

This model and our observations suggest a range of emission mitigation opportunities. Maintaining lower surplus mineral-N in the soil decreases N_2O emissions, and has potential to completely eliminate emissions below the threshold value for the clay soil (70 mg [kg of soil]$^{-1}$). Plant uptake (including crops and managed pastures) would constantly act to decrease the mineral-N resident

at any time, and may provide a viable and cost-effective tool to decrease emissions.

This discussion of scenarios is a simplification. Peak emission moisture conditions at this site are concentrated in the summer months. Also, where temperatures are substantially different, a temperature dependent extension is required, or calibration for a specific temperature range. A raft of approaches are likely to be effective in this respect (e.g. Shaffer et al., 1991; Xu et al., 1998). There also remains the need for field validation to test these findings at a larger scale.

The IPCC default emission factor for secondary N_2O is 1% (uncertainty range = 0.2%—5%) of N added. However, the sharp threshold relationship determined for N_2O emission and resident mineral-N (70 mg [kg of soil]$^{-1}$) highlights a fundamental flaw in the IPCCs current approach to predicting indirect N_2O emissions: i.e. these emissions aren't controlled primarily by N deposition rates but instead by the amount of mineral-N remaining in the soil (the sum of deposition and pre-existing mineral-N). This finding is very important as it opens the potential to develop a soil-based process understanding approach that allows prediction of N_2O emissions from N-sources added to agricultural soils (Fig. 6b). Field validation of the modelling approach described here (equation (4)) may allow more rigorous, country specific determination of the IPCC emission factors for both direct and indirect emissions.

An improved management-responsive approach to inventory estimation, in addition to achieving greater calculation accuracy, would have other benefits. It may also provide an incentive for improved management. The model fitted here (equation (4)) suggests that for a range of management scenarios and region specific conditions emissions are likely to be larger or less than indicated by the inventory emission factor (1% of deposited N emitted as N_2O, IPCC, 2006). This type of simple modelling approach could form the basis of a more region specific and management responsive inventory protocol.

5. Conclusions

Emission values contributed a detailed three dimensional landscape representing the dependence of N_2O emissions on WFPS and mineral-N. Emissions from the vertisol (i.e., the clay soil) peaked from 85 to 93% WFPS ($<0.002 \mu g$ N [g soil]$^{-1}$ min^{-1}), increasing as resident mineral-N increased, up to a plateau. Substantial communities of bacterial nitrifiers were present at the peak emission conditions but bacterial denitrifiers made up a larger proportion of the community. Fungal denitrifiers were less prevalent. Emissions of N_2O from the sandy soil peaked at a lower WFPS (about 60%; $<5 \times 10^{-5}$ g N [g soil]$^{-1}$ min^{-1}), with an indistinct relationship with increasing resident mineral N. This difference was associated with strong conversion of added NH_4^+ to NO_3^- in the clay soil, but poor conversion in the sandy soil. Sandy soil N_2O emissions were only a few percent of clay soil emissions, mirroring the much lower biological activity of this soil.

A process-based, mathematical model incorporating a relationship involving soil NO_3^- (where all added NH_4^+ was assumed to be nitrified) and a moisture stress function was well suited to the clay soil data ($R^2 = 90$%). This function was not well suited to the sandy soil, where nitrification was much less complete. Preliminary investigations of a relationship representing mineral-N pools (NO_3^- and NH_4^+) was conducted but further investigation is required.

A threshold effect was observed in the vertisol where resident mineral-N did not result in increased N_2O emissions until concentrations exceeded a threshold concentration (about 0.07 mg (g of soil)$^{-1}$), indicating potential for managements that minimise N_2O emission.

The model (equation (4)) fitted to the clay soil data suggests that in a range of scenarios emissions can be greater than, or substantially less than, indicated by the current inventory approach under different regional and management conditions. This management responsive emission calculation approach could provide a more effective incentive for improved nutrient management.

References

Abalos, D., Sanz-Cobena, A., Garcia-Torres, L., van Groenigen, J.W., Vallejo, A., 2013. Role of maize stover incorporation on nitrogen oxide emissions in a non-irrigated Mediterranean barley field. Plant and Soil 364, 357—371. http://dx.doi.org/10.1007/s11104-012-1367-4.

Abbasi, M.K., Adams, W.A., 1998. Loss of nitrogen in compacted grassland soil by simultaneous nitrification and denitrification. Plant and Soil 200, 265—277. http://dx.doi.org/10.1023/A:1004398520150.

Allen, A.G., Harrison, R.M., Erisman, J.-W., 1989. . Field measurements of the dissociation of ammonium nitrate and ammonium chloride aerosols. Atmospheric Environment (1967) 23, 1591—1599. http://dx.doi.org/10.1016/0004-6981(89)90418-6.

Anthonisen, A.C., Loehr, R.C., Prakasam, T.B.S., Srinath, E.G., 1976. Inhibition of nitrification by ammonia and nitrous acid. Journal of Water Pollution Control Federation 48, 835—852.

Ball, B.C., Horgan, G.W., Clayton, H., Parker, J.P., 1997. Spatial variability of nitrous oxide fluxes and controlling soil and topographic properties. Journal of Environmental Quality 26, 1399—1409.

Bates, D.M., Watts, D.G., 2007. Nonlinear Regression Analysis and its Applications. John Wiley & Sons, New York.

Berendse, F., Laurijsen, C., Okkerman, P., 1988. The acidifying effect of ammonia volatilized from farm-manure on forest soils. Ecological Bulletins 136—138. http://dx.doi.org/10.2307/20113011.

Bouwman, A., 1998. Environmental science — nitrogen oxides and tropical agriculture. Nature 392, 866—867. http://dx.doi.org/10.1038/31809.

Brochier-Armanet, C., Boussau, B., Gribaldo, S., Forterre, P., 2008. Mesophilic crenarchaeota: proposal for a third archaeal phylum, the Thaumarchaeota. Nature Reviews Microbiology 6, 245—252. http://www.nature.com/nrmicro/journal/v6/n3/suppinfo/nrmicro1852_S1.html.

Brumme, R., Borken, W., Finke, S., 1999. Hierarchical control on nitrous oxide emission in forest ecosystems. Global Biogeochemical Cycles 13, 1137—1148. http://dx.doi.org/10.1029/1999GB900017.

Butterbach-Bahl, K., Gasche, R., Breuer, L., Papen, H., 1997. Fluxes of NO and N_2O from temperate forest soils: impact of forest type, N deposition and of liming on the NO and N_2O emissions. Nutrient Cycling in Agroecosystems 48, 79—90. http://dx.doi.org/10.1023/A:1009785521107.

Butterbach-Bahl, K., Baggs, E.M., Dannenmann, M., Kiese, R., Zechmeister-Boltenstern, S., 2013. Nitrous oxide emissions from soils: how well do we understand the processes and their controls? Philosophical Transactions of the Royal Society B: biological Sciences 368. http://dx.doi.org/10.1098/rstb.2013.0122.

Caporaso, J.G., Caporaso, J.G., Kuczynski, J., Stombaugh, J., Bittinger, K., 2010. QIIME allows analysis of high-throughput community sequencing data. Nature Methods 7, 335—336. http://dx.doi.org/10.1038/NMETH.F.303.

Corre, M.D., Pennock, D.J., Kessel, C.V., Kirkeliott, D., 1999. Estimation of annual nitrous oxide emissions from a transitional grassland-forest region in Saskatchewan, Canada. Biogeochemistry 44, 29—49. http://dx.doi.org/10.1007/BF00992997.

Daims, H., 2014. The family nitrospiraceae. In: Rosenberg, E., DeLong, E., Lory, S., Stackebrandt, E., Thompson, F. (Eds.), The Prokaryotes. Springer Berlin Heidelberg, pp. 733—749.

Dalal, R.C., Wang, W.J., Robertson, G.P., Parton, W.J., 2003. Nitrous oxide emission from Australian agricultural lands and mitigation options: a review. Australian Journal of Soil Research 41, 165—195.

Davidson, E.A., Rogers, J., Whitman, W., others, 1991. Fluxes of Nitrous Oxide and Nitric Oxide from Terrestrial Ecosystems. In: Microbial Production and Consumption of Greenhouse Gases: Methane, Nitrogen Oxides, and Halomethanes, pp. 219—235.

Davidson, E.A., Keller, M., Erickson, H.E., Verchot, L.V., Veldkamp, E., 2000. Testing a Conceptual Model of Soil Emissions of Nitrous and Nitric Oxides: using two functions based on soil nitrogen availability and soil water content, the hole-in-the-pipe model characterizes a large fraction of the observed variation of nitric oxide and nitrous oxide emissions from soils. BioScience 50, 667—680.

Denier van der Gon, H., Bleeker, A., 2005. Indirect N$_2$O emission due to atmospheric N deposition for the Netherlands. Atmospheric Environment 39, 5827–5838. http://dx.doi.org/10.1016/j.atmosenv.2005.06.019.

DeSantis, T.Z., Hugenholtz, P., Larsen, N., Rojas, M., Brodie, E.L., Keller, K., Huber, T., Dalevi, D., Hu, P., Andersen, G.L., 2006. Greengenes, a chimera-checked 16S rRNA gene database and workbench compatible with ARB. Applied and Environmental Microbiology 72, 5069–5072.

Dobbie, K.E., Smith, K.A., 2001. The effects of temperature, water-filled pore space and land use on N$_2$O emissions from an imperfectly drained gleysol. European Journal of Soil Science 52, 667–673.

Edgar, R.C., 2010. Search and clustering orders of magnitude faster than BLAST. Bioinformatics 26, 2460–2461. http://dx.doi.org/10.1093/bioinformatics/btq461.

Edgar, R.C., Haas, B.J., Clemente, J.C., Quince, C., Knight, R., 2011. UCHIME improves sensitivity and speed of chimera detection. Bioinformatics 27, 2194–2200.

Firestone, M., Davidson, E., Andreae, M., Schimel, D., 1989. Microbiological basis of NO and N2O production and consumption in soil. In: Exchange of Trace Gases between Terrestrial Ecosystems and the Atmosphere. John Wiley & Sons, p. 721.

Fowler, D., Fowler, D., Pitcairn, C.E., Sutton, M., Flechard, C., 1998. The mass budget of atmospheric ammonia in woodland within 1 km of livestock buildings. Environmental Pollution (1987) 102, 343–348. http://dx.doi.org/10.1016/S0269-7491(98)80053-5.

Gee, G.W., Bauder, J.W., 1986. Particle-size analysis. In: Klute, A. (Ed.), Methods of Soil Analysis. Part 1 — Physical and Mineralogical Methods. American Society of Agronomy, Madison, Wisconsin, pp. 383–411.

Giles, M., Morley, N., Baggs, E.M., Daniell, T.J., 2012. Soil nitrate reducing processes drivers, mechanisms for spatial variation, and significance for nitrous oxide production. Frontiers in Microbiology 3, 407. http://dx.doi.org/10.3389/fmicb.2012.00407.

Gilks, W.R., Richardson, S., Spiegelhalter, D.J., 1996. Markov Chain Monte Carlo in Practice.

Hawkins, S., Robinson, K., Layton, A., Sayler, G., 2010. Limited impact of free ammonia on Nitrobacter spp. inhibition assessed by chemical and molecular techniques. Bioresource Technology 101, 4513–4519. http://dx.doi.org/10.1016/j.biortech.2010.01.090.

Intergovernmental Panel on Climate Change, 2006. IPCC — Task Force on National Greenhouse Gas Inventories [WWW Document]. URL. http://www.ipcc-nggip.iges.or.jp/public/2006gl/vol4.html (accessed 22.04.14).

Isbell, R.F., 2002. The Australian Soil Classification, Australian Soil and Land Survey Handbook. CSIRO Publishing, Collingwood, Victoria, Australia.

Khalil, K., Mary, B., Renault, P., 2004. Nitrous oxide production by nitrification and denitrification in soil aggregates as affected by O$_2$ concentration. Soil Biology and Biochemistry 36, 687–699. http://dx.doi.org/10.1016/j.soilbio.2004.01.004.

Koehler, B., Corre, M., Steger, K., Well, R., Zehe, E., Sueta, J., Veldkamp, E., 2012. An in-depth look into a tropical lowland forest soil: nitrogen-addition effects on the contents of N$_2$O, CO$_2$ and CH$_4$ and N$_2$O isotopic signatures down to 2-m depth. Biogeochemistry 111, 695–713. http://dx.doi.org/10.1007/s10533-012-9711-6.

Koljalg, U., Larsson, K.H., Abarenkov, K., Nilsson, R.H., Alexander, I.J., Eberhardt, U., Erland, S., Hoiland, K., Kjoller, R., Larsson, E., Pennanen, T., Sen, R., Taylor, A.F.S., Tedersoo, L., Vralstad, T., Ursing, B.M., 2005. UNITE: a database providing web-based methods for the molecular identification of ectomycorrhizal fungi. New Phytologist 166, 1063–1068. http://dx.doi.org/10.1111/j.1469-8137.2005.01376.x.

Li, Y., White, R., Chen, D.L., Zhang, J.B., Li, B.G., Zhang, Y.M., Huang, Y.F., Edis, R., 2007. A spatially referenced water and nitrogen management model (WNMM) for (irrigated) intensive cropping systems in the North China Plain. Ecological Modelling 203, 395–423. http://dx.doi.org/10.1016/j.ecolmodel.2006.12.011.

Linn, D.M., Doran, J.W., 1984. Effect of water-filled pore space on carbon dioxide and nitrous oxide production in tilled and nontilled soils. Soil Science Society of America Journal 48, 1267–1272. http://dx.doi.org/10.2136/sssaj1984.03615995004800060013x.

Mary, B., Recous, S., Robin, D., 1998. A model for calculating nitrogen fluxes in soil using N-15 tracing. Soil Biology & Biochemistry 30, 1963–1979. http://dx.doi.org/10.1016/S0038-0717(98)00068-6.

McGinn, S.M., Janzen, H.H., Coates, T., 2003. Atmospheric ammonia, volatile fatty acids, and other odorants near beef feedlots. Journal of Environmental Quality 32, 1173–1182. http://dx.doi.org/10.2134/jeq2003.1173.

Philippot, L., Hallin, S., Schloter, M., 2007. Ecology of denitrifying prokaryotes in agricultural soil. In: Donald, L.S. (Ed.), Advances in Agronomy. Academic Press, pp. 249–305.

Pieiro, G., Perelman, S., Guerschman, J.P., Paruelo, J.M., 2008. How to evaluate models: observed vs. predicted or predicted vs. observed? Ecological Modelling 216, 316–322. http://dx.doi.org/10.1016/j.ecolmodel.2008.05.006.

Pilinis, C., Seinfeld, J.H., 1987. Continued development of a general equilibrium model for inorganic multicomponent atmospheric aerosols. Atmospheric Environment (1967) 21, 2453–2466. http://dx.doi.org/10.1016/0004-6981(87)90380-5.

Pratt, C., Redding, M., Hill, J., Shilton, A., Chung, M., Guieysse, B., 2015. Good science for improving policy: greenhouse gas emissions from agricultural manures. Animal Production Science 55, 691–701.

Python Software Foundation, 2014. Python programming Language Version 2.7.10 [WWW Document]. URL. https://www.python.org/ (accessed 26.05.15).

R Core Team, 2012. R: a Language and Environment. Gnu Software License. http://www.gnu.org/software/r/R.html.

Rayment, G.E., Lyons, D.J., 2010. Soil Chemical Methods — Australasia.

Redding, M.R., Devereux, J., Phillips, F., Lewis, R., Naylor, T., Kearton, T., Hill, C.J., Weidemann, S., 2015. Field measurement of beef pen manure methane and nitrous oxide reveals a surprise for inventory calculations. Journal of Environmental Quality 44, 720–728. http://dx.doi.org/10.2134/jeq2014.04.0159.

Sanz-Cobena, A., Snchez-Martn, L., Garca-Torres, L., Vallejo, A., 2012. Gaseous emissions of N$_2$O and NO and NO$_3$ leaching from urea applied with urease and nitrification inhibitors to a maize (Zea mays) crop. Agriculture. Ecosystems & Environment 149, 64–73. http://dx.doi.org/10.1016/j.agee.2011.12.016.

Senbayram, M., Chen, R., Mhling, K.H., Dittert, K., 2009. Contribution of nitrification and denitrification to nitrous oxide emissions from soils after application of biogas waste and other fertilizers. Rapid Communications in Mass Spectrometry 23, 2489–2498. http://dx.doi.org/10.1002/rcm.4067.

Shaffer, M.J., Halvorson, A.D., Pierce, F.J., 1991. Nitrate leaching and economic analysis package (NLEAP): model description and application. In: Managing Nitrogen for Groundwater Quality and Farm Profitability. Soil Science Society of America, Madison, WI, pp. 285–322.

Soil Survey Staff, 1998. Keys to Soil Taxonomy, eighth ed. United Sates Department of Agriculture, Natural Resource Conservation Service, Washington, D.C.

Staebler, R.M., McGinn, S.M., Crenna, B.P., Flesch, T.K., Hayden, K.L., Li, S., 2009. Three-dimensional characterization of the ammonia plume from a beef cattle feedlot. Atmospheric Environment 43, 6091–6099. http://dx.doi.org/10.1016/j.atmosenv.2009.08.045.

Stehfest, E., Bouwman, L., 2006. N$_2$O and NO emission from agricultural fields and soils under natural vegetation: summarizing available measurement data and modeling of global annual emissions. Nutrient Cycling in Agroecosystems 74, 207–228. http://dx.doi.org/10.1007/s10705-006-9000-7.

Swerts, M., Merckx, R., Vlassak, K., 1996. Influence of carbon availability on the production of NO, N$_2$O, N$_2$, and CO$_2$ by soil cores during anaerobic incubation. Plant and Soil 181, 145–151.

Todd, R.W., Cole, N.A., Clark, R.N., Flesch, T.K., Harper, L.A., Baek, B.H., 2008. Ammonia emissions from a beef cattle feedyard on the southern High Plains. Atmospheric Environment 42, 6797–6805. http://dx.doi.org/10.1016/j.atmosenv.2008.05.013.

The Mathworks Inc, 2012. Matlab. The MathWorks Inc., Natick, Massachusetts.

Tsuruta, S., Takaya, N., Zhang, L., Shoun, H., Kimura, K., Hamamoto, M., Nakase, T., 1998. Denitrification by yeasts and occurrence of cytochrome P450nor in Trichosporon cutaneum. Fems Microbiology Letters 168, 105–110. http://dx.doi.org/10.1016/s0378-1097(98)00427-3.

Walkley, A., Black, I., 1934. An examination of the Degtjareff method for determining soil organic matter and a proposed modification of the chromic acid titration method. Soil Science 37, 29–38.

Watson, S.W., Bock, E., Harms, H., Koops, H.P., Hooper, A., 1989. Nitrifying bacteria. In: Staley, J.T., Bryant, M.P., Pfennig, N., Holt, J.G. (Eds.), Bergeys Manual of Systematic Bacteriology. Williams and Wilkins Co., Baltimore, USA, pp. 1808–1834.

Wexler, A.S., Seinfeld, J.H., 1990. The distribution of ammonium salts among a size and composition dispersed aerosol. Atmospheric Environment. Part A. General Topics 24, 1231–1246. http://dx.doi.org/10.1016/0960-1686(90)90088-5.

Xu, C., Shaffer, M.J., Al-kaisi, M., 1998. Simulating the impact of management practices on nitrous oxide emissions. Soil Science Society of America Journal 62, 736–742.

Yang, R., Ti, C., Li, F., Deng, M., Yan, X., 2010. Assessment of N$_2$O NO$_x$ and NH$_3$ emissions from a typical rural catchment in Eastern China. Soil Science and Plant Nutrition 56, 86–94. http://dx.doi.org/10.1111/j.1747-0765.2010.00459.x.

Zanner, C.W., Bloom, P.R., 1995. Mineralization, nitrification, and denitrification in histosols of Northern Minnesota. Soil Science Society of America Journal 59, 1505–1511. http://dx.doi.org/10.2136/sssaj1995.03615995005900050042x.

Zhang, J., Kobert, K., Flouri, T., Stamatakis, A., 2014. PEAR: a fast and accurate Illumina Paired-End reAd mergeR. Bioinformatics (Oxford, England) 30, 614–620.